27th EPS Conference on Contr. Fusion and Plasma Phys. Budapest, 12-16 June 2000 ECA Vol. **24B** (2000) 488 -491

3D Finite Larmor Radius Guiding Center Model of a Plasma Edge

W. Entler[*], G. Kamelander[*] and M. Shoucri[**]

[*] *Österreichisches Forschungszentrum Seibersdorf, Austria*
[**] *Centre canadien de fusion magnétique Varennes, Québec, Canada*

This work has been performed in Euratom-ÖAW-Association

Introduction

The turbulent evolution of a 3D guiding center plasma at the plasma edge was simulated using an Eulerian Vlasov code, which has been parallelized on a parallel computer. The plasma edge is represented by a three dimensional cartesian plasma layer, where the *x* direction corresponds to the poloidal periodic direction, the *y* direction to the radial nonperiodic direction and the *z* direction to the toroidal periodic direction. The magnetic field $\vec{B}$ is regarded as constant and is situated in the *xz*-plane making an angle of 89.5° with the *x*-axis (see Fig. 1). The model includes the $\vec{E}\times\vec{B}$-drift. Due to the spatial dimensions of the plasma layer finite larmor radius (FLR) effects must incorporated into the model. The FLR correction procedure [1] applied leads to a charge separation at the plasma edge, which is accentuated by the polarization drift.

Pertinent Equations

The electrons are represented by their guiding center distribution function $f_e(x,y,z,v_{//})$, which is depending on three spatial coordinates x,y,z and the velocity $v_{//}$ parallel to the magnetic field $\vec{B}$. The ions are given by the guiding center density $n_i(x,y,z)$. The temporal evolution of these quantities is determined by the electron gyrokinetic equation,

$$\frac{\partial f_e}{\partial t}+\vec{\nabla}\cdot\left(\vec{u}_e f_e\right)+v_{//}\hat{b}\cdot\vec{\nabla}f_e-\frac{e}{m_e}E_{//}\frac{\partial f_e}{\partial v_{//}}=0 \qquad \textbf{(1)}$$

and the ion gyrofluid continuity equation

$$\frac{\partial n_i}{\partial t}+\vec{\nabla}\cdot\left(\vec{u}_i^{\,*}n_i\right)=0 \qquad \textbf{(2)}$$

where $\vec{u}_e$ and $\vec{u}_i^*$ are the total drift velocities of electrons, for which the polarisation drift is neglected, and the ions, respectively.

$$\vec{u}_e = \vec{u}_{de} = \frac{\vec{E}\times\vec{B}}{B^2}, \quad \vec{u}_i^* = \vec{u}_{di}^* + \vec{u}_{pi}^* = \frac{\vec{E}^*\times\vec{B}}{B^2} + \frac{1}{\omega_{ci}B}\left(\frac{\partial\vec{E}_\perp^*}{\partial t} + \vec{u}_{di}^*\cdot\vec{\nabla}\vec{E}_\perp^*\right) \tag{3}$$

The other symbols used are the unity vector $\hat{b}$ in the magnetic field direction, the elementary charge e, the electron mass m_e, the electric field $\vec{E}$ and the ion larmor frequency ω_{ci}. As can be seen from equation (2), the motion of the heavy ions parallel to $\hat{b}$ is neglected. The guiding center equations are coupled by the poisson equation.

$$\vec{\nabla}^2\Phi = -\frac{e}{\varepsilon_0}\left(n_i^* - n_e\right), \quad n_e = \int f_e\, dv_{//} \tag{4}$$

The stars in the equations (2) to (4) indicate the finite larmor radius (FLR) correction of the corresponding quantity. Using the fourier components $A_{\vec{k}}$ of $A(\vec{r})$ this operation can be written as

$$A^*(\vec{r}) = \sum_{\vec{k}} A_{\vec{k}}\exp\left(i\vec{k}\cdot\vec{r}\right)g_{\vec{k}}, \quad g_{\vec{k}} = \exp\left(-\frac{r_c^2\,k_\perp^2}{2}\right) \tag{5}$$

where r_c denotes the larmor radius and $k_\perp$ is the component of $\vec{k}$ perpendicular to $\hat{b}$.

Initial Values and Parameters

The initial electron distribution function f_e and ion density n_i, respectively, are given by

$$n_i(t=0) = n_0(y)\cdot\Delta_x\cdot\Delta_z, \quad f_e(t=0) = n_0(y)\cdot\Delta_x\cdot\Delta_z\,\frac{\exp\left(\frac{-v_{//}^2}{2T_e(y)}\right)}{\sqrt{2\pi T_e(y)}} \tag{6}$$

where

$$\Delta_x = 1+\varepsilon_x\sin k_{0x}x + \varepsilon_x\sin 2k_{0x}x + \varepsilon_x\sin 3k_{0x}x, \Delta_z = 1+\varepsilon_z\sin k_{0z}z + \varepsilon_z\sin 2k_{0z}z + \varepsilon_z\sin 3k_{0z}z \tag{7}$$

$$n_0(y) = \frac{1}{2}\left(1+\tanh(1.6\cdot y)\right), \quad T_e(y) = 0.2 + 0.4\cdot\left(1+\tanh(1.6\cdot y)\right) \tag{8}$$

$$k_{0x} = \frac{2\pi}{L_x}, k_{0z} = \frac{2\pi}{L_z}, \quad \frac{m_i}{m_e} = 1840, \quad \frac{\omega_{ci}}{\omega_{pi}} = \frac{\lambda_D}{r_{ci}} = 0.9 \tag{9}$$

$$L_x = 28\lambda_D, \quad L_y = 12\lambda_D, \quad L_z = 80\lambda_D, \quad L_v = 10\,v_{th,e} \tag{10}$$

The number of grid points used was $N_x = N_y = N_z = N_v = 64$. For the initial perturbation $\varepsilon_x = 0.002$, $\varepsilon_z = 0$ for run 1 and $\varepsilon_z = 0.0002$ for run 2 was chosen.

Results

Due to the different larmor radius of ions and electrons the density gradient at the plasma edge results in a charge separation, which is reproduced by the FLR correction operation in the model. The resulting inhomogen electric field E_y (see Figure 5) in radial direction leads to the formation of $\vec{E} \times \vec{B}$ -drift and thus to a shear in the transverse drift velocity u_x. The growth rates of the Kelvin-Helmholtz instability driven by this velocity shear have been studied before in models with two spatial dimensions x and y [2]. Figure 2 shows the temporal evolution of the fourier modes k_{0x} to $4k_{0x}$ of the potential Φ spatially averaged over y and z. Due to the rapid motion of the electrons along the magnetic field lines, which now is included in the three dimensional model, the modes saturate at a lower level than observed in the two dimensional model [2]. Figure 3 shows the temporal evolution of the potential modes k_{0z} to $4k_{0z}$. At t~8000 there is a sudden growth of these modes. It can be noticed that the saturation level reached after the growth phase and the moment at which it occurs is the same for run 1, where the modes were not initially perturbed and run 2 with ε_z=0.0002. As also can be seen from Figure 3, the saturation level reached by the z potential modes is low compared to the x potential modes in Figure 2. Development towards saturation and large structures can also be observed in Figure 4, where the potential profile, obtained by averaging over x and z is shown for different times t. The profile of the electric field E_y is shown in Figure 5. Figure 6 shows the profiles of the electron density n_e and the FLR corrected ion density n_i^*. The charge density ρ appearing in the poisson equation (4) is calculated by $n_i^* - n_e$, reproducing the charge separation mentioned above.

References

[1] G. Knorr et al., Finite Larmor Radius Effects to Arbitrary Order, Physica Scripta 38, 82-834, 1988

[2] G. Manfredi et al., Charge Separation and Velocity Shear at a Plasma Edge in The Finite Gyro-Radius Guiding Center Approximation, Physica Scripta 58, 159-172, 1998

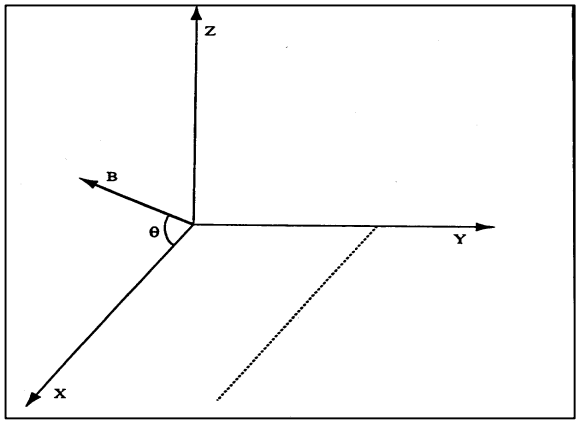

Figure 1 : Slab geometry

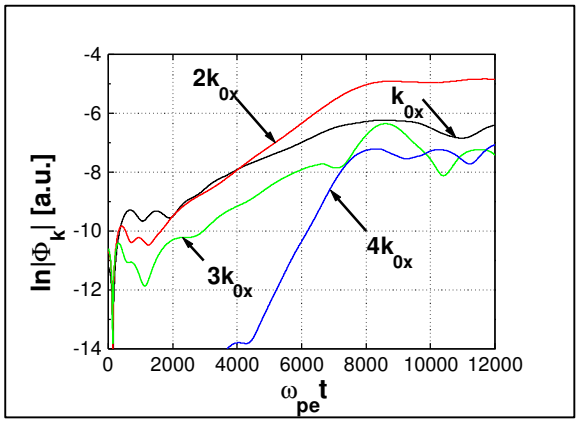

Figure 2 : Potential modes in x direction

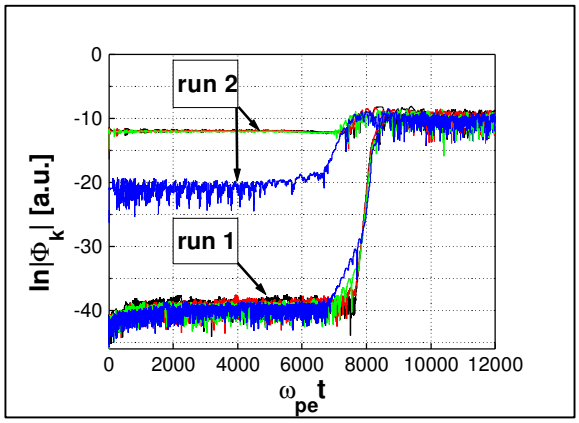

Figure 3 : Potential modes in z direction

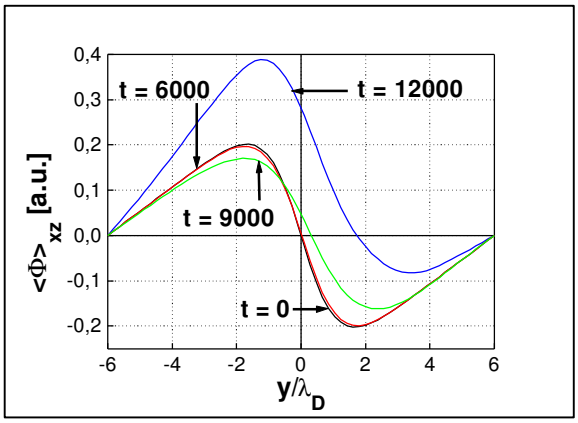

Figure 4 : Temporal evolution of the potential

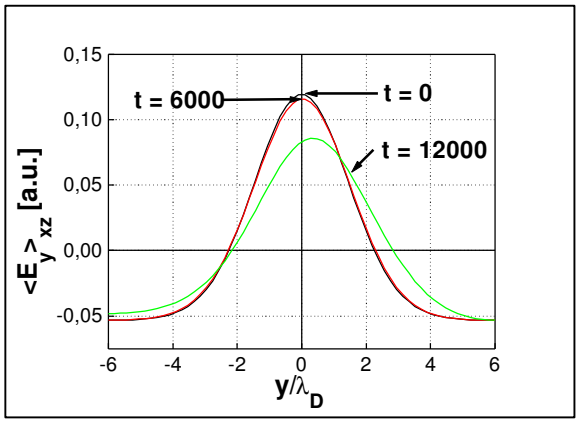

Figure 5 : Temporal evolution of E_y

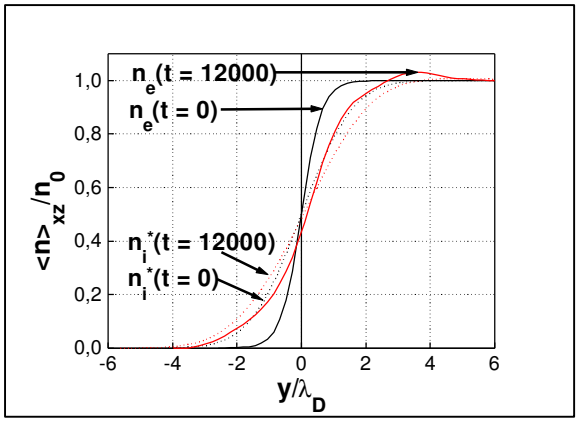

Figure 6 : Temporal evolution of the ion density